https://doi.org/10.5194/egusphere-2025-3664
Preprint. Discussion started: 8 August 2025

Targeted Teleconnections and their Application to the Postprocessing of Climate Predictions

Clementine Dalelane[1], Andreas Paxian[1], Martín Senande[4], Sabela Sanfiz[2], Estéban Rodríguez Guisado[2], Jan Wandel[1], and Abhinav Tyagi[3]

[1]Deutscher Wetterdienst (DWD), Frankfurter Str. 135, Offenbach, Germany
[2]Agencia Estatal de Meteorología (AEMET), C/ Leonardo Prieto Castro, 8, Ciudad Universitaria, Madrid, Spain
[3]Fraunhofer Institute for Energy Economics and Energy System Technology (IEE), Joseph–Beuys–Straße 8, Kassel, Germany
[4]Mitiga Solutions, Carrer de Julia Portet, 3, 08002 Barcelona, Spain

Correspondence: Clementine Dalelane (clementine.dalelane@dwd.de)

Abstract. The demand for skillful climate predictions on subseasonal-to-multidecadal time scales is rising almost by the day, not least because the growing renewable energy sector, but also many other important socio–economic sectors are vulnerable to climate variations. Large scale atmospheric patterns in the North–Atlantic European sector, so-called teleconnections, are well known to have major influence on European climate conditions. For that reason there exists a wide variety of hybrid dynamical–statistical applications, which combine dynamical model output with teleconnections in one way or another to improve the rather modest predictive skill of state-of-the-art dynamical climate forecasts over Europe. The potential improvement generated by these kinds of postprocessing methods is naturally limited by the strength of association between the circulation patterns and the local climate parameters. We propose a statistical technique to retrieve atmospheric patterns—targeted teleconnections—that are maximally predictive for a given climate parameter in a region of choice so as to optimize the potential of statistical postprocessing. The possibility of improvement in forecast skill induced by the implementation of targeted teleconnections is demonstrated in four applications.

1 Introduction

With the development of increasingly reliable climate models, operational climate predictions from subseasonal to multi-decadal time scales are starting to flourish all across national meteorological agencies, coordinated by multi-national and global organisations like the Copernicus Climate Change Service (C3S) and the World Meteorological Organisation. Unlike numerical weather prediction, climate prediction aims at forecasting atmospheric conditions which lie beyond the deterministic prediction horizon and reach well into the realms of atmospheric chaos. Nevertheless boundary conditions with low frequency variability strongly modulate circulation, and owing to their slow variability, their influence transmits a certain predictability (Hall et al., 2019; Strommen et al., 2023; Sun et al., 2024). Circulation, in turn, has strong impacts on the down stream surface climate, albeit to varying extent depending on parameter, region and season (Cionni et al., 2022; Simpson et al., 2024). The emphasis here is on surface *climate* as the effects are manifest not in single events, but rather in the probability distributions of their generation and evolution.

https://doi.org/10.5194/egusphere-2025-3664
Preprint. Discussion started: 8 August 2025

We are therefore able to identify a causal chain leading from the persistent, partially predictable boundary conditions, first and foremost the ocean, but also cryoshere, stratosphere, and land surface, to sensible climate like 2m temperature (T2M), precipitation (PR), wind speed, and radiation (Simpson et al., 2019). The crucial link in this causal chain, notwithstanding feedback loops, is the atmospheric circulation, which, turbulent though it is on all scales, appears to be self-organizing in semi-persistent and recurrent patterns (Hannachi et al., 2017; Faranda et al., 2017; Strommen et al., 2022). The circulation, its main feature over the North–Atlantic European (NAE) sector being the eddy-driven jet stream (Perez et al., 2024), is usually measured by means of mean sea level pressure (MSLP) or geopotential height at 500 hPa (ZG500) patterns and has long been the object of extensive study (Feldstein and Franzke, 2017). One very efficient, even though linear, way of summarizing the low-dimensional manifold character of the circulation is Principal Component Analysis (PCA), also known in atmospheric sciences as Empirical Orthogonal Function (EOF) Analysis (Hannachi, 2021). Focusing on the NAE sector, it has been conclusively shown that the four dominant circulation patterns describing the location of blocking highs in the sector—namely the North Atlantic Oscillation (NAO), the East Atlantic pattern (EA), the East Atlantic/West Russia Pattern (EAWR) and the Scandinavian Pattern (SCA)—represent the largest part of the variability of the regional large scale circulation, and are strongly correlated to a wide variety of local climate variables in Europe (Cionni et al., 2022; Simpson et al., 2024). Maybe it was this long distance-relationship, which has won them the alternative name of "teleconnection".

The teleconnections between circulation and local climate are widely exploited in statistical climatology with one major application being the statistical postprocessing of climate predictions. Although the reliability of climate predictions has made enormous progress in recent decades, there still remain large swaths of the globe where state-of-the-art dynamical climate models struggle to deliver decision-relevant climate forecasts, among them Europe (Dorrington et al., 2020). Statistical post-processing of model output is one of the provisional remedies to such inconveniences, which is capable of improving the predictive skill of the forecasts. The techniques, that rely heavily on knowledge about teleconnections, can roughly be divided into two main categories, depending on the problem that is identified at the core of this mishap.

It is often the case that a dynamical model presents reasonable skill in predicting the large-scale circulation patterns (Schuhen et al., 2022), but this skill is somehow lost on its way from the circulation to the surface variables. Under these circumstances, a viable workaround can be the substitution of surface variable model output fields by statistical reconstructions of the fields in question based on observations conditioned on state of the circulation forecast by the model. This approach is often termed statistical downscaling, it has found widespread application also in the European domain and is applicable both to local climate fields like T2M and PR and to derived parameters, e. g. run-off and renewable energy production (Rodríguez-Guisado et al., 2019; Bloomfield et al., 2021; Ramón et al., 2021; Bett et al., 2022; Cionni et al., 2022; Golian et al., 2022; Tsartsali et al., 2023; Rouges et al., 2024).

We acknowledge that recently there is a floury of downscaling models based on machine learning (ML) as allegedly opposed to "traditional" methods. But ML is just another name for statistics, if anything it is a highly nonlinear and consequently very data intensive branch, and the applications suffer from similar limitations (Hernanz et al., 2024). Therefore we deem such distinctions meaningless.

https://doi.org/10.5194/egusphere-2025-3664
Preprint. Discussion started: 8 August 2025

The other configuration, one which is typically found in the North Atlantic in autumn and winter, is the overdispersive forecast with wide ensemble spread and low predictive skill in forecasting the atmospheric patterns (the so-called signal-to-noise paradox, see Scaife and Smith (2018)), while the simultaneous teleconnection between circulation and surface climate within the ensemble members is reasonably realistic. The wide ensemble spread opens an opportunity to select or weigh the forecast members according to a more reliable prediction of the circulation indices based on the initial state of the boundary conditions, if available. This so-called ensemble subsampling or weighting is being increasingly implemented by European climate services (Dobrynin et al., 2018; Sánchez-García et al., 2019; Dalelane et al., 2020; Benassi et al., 2024). The reliable prediction of the circulation indices, on which this whole procedure is based upon, can itself be a dynamical model forecast like a (multi-model) ensemble mean, or a statistical (including ML) prediction that exploits the relationship between the initial boundary conditions and the circulation (Hall et al., 2019; Dalelane et al., 2020; Sun et al., 2024).

In both promising cases, the teleconnection between the circulation indices and the surface variables is crucial to the success of the postprocessing, the stronger the better. Unfortunately, the strength of those teleconnections is far from uniform, spatially and temporally (e.g. Bednorz et al. (2019); West et al. (2022)). And having to account for four circulation indices at any one time can considerably limit the feasibility and the statistical robustness of both approaches. It would therefore be desirable to concentrate as much dependence as possible in the smallest possible number of indices.

Let us briefly return to the starting point of our discussion, which was the construction of the circulation patterns/indices. There we discover that there exists a great number of PCA-related techniques, some of which are specifically designed to capture the association between two blocks of variables. One of them, Partial Least Squares (PLS) regression, explicitly models a regression relationship between a block of predictor variables and a block of response variables. The resulting patterns/indices are meant to strike a balance between reducing the dimension of the predictor variables and predicting the response variables efficiently. This very feature will facilitate the kind of postprocessing methods that we are considering in our study. As these circulation patterns/indices are constructed so as to maximize the teleconnection to a target variable, hence their suggested name “targeted teleconnections”.

Nevertheless, a warning is appropriate at this point that the targeted teleconnections must not be misintepreted as physical modes of the circulation variability. They are in contrast the modes of covariability, which exert the strongest influence from the circulation to the target. They can and will differ from the EOF-derived circulation patterns. Just as the teleconnections to one target will differ from the teleconnections to another target.

Recently, a few publications have elaborated on similar ideas. Baker et al. (2018) and Bloomfield et al. (2020) were able to improve their prediction of seasonal precipitation in various regions of the British Isles by means of a targeted circulation index, derived from the correlation maps between PR in Britain and MSLP in the NAE sector. Goutham et al. (2023), in contrast, replaced the traditional EOF circulation indices in his statistical downscaling application by indices based on redundancy analysis (RDA) to achieve a substantial increase in subseasonal prediction skill for T2M and 100m wind speed. Spuler et al. (2024)’s targeted weather regimes conducive to Moroccan extreme rainfall pursue a somewhat similar approach on a subseasonal-to-seasonal timescale, this time by means of a regression-mixture model variational autoencoder. These are to our best knowledge the only applications of targeted circulation patterns in climate prediction so far.

https://doi.org/10.5194/egusphere-2025-3664
Preprint. Discussion started: 8 August 2025

Of course, there is nowadays the breathtaking development of purely data driven climate modeling relying on deep neural networks (Watt-Meyer et al., 2023; Kochkov et al., 2024). Apart from still lacking the coupling to data driven ocean, cryosphere and land components, these models' basic concept is the emulation of reanalyses and/or coupled global circulation models (GCM), because they are not yet capable of extracting physically consistent forecasts from the available short, scarce and noisy observational data record alone. So directly or indirectly, dynamical climate models are still indispensable for doing the heavy lifting in climate prediction, at least up until today.

On the other hand, there are direct statistical climate prediction models specialized on one specific, often very narrow target variable like the ENSO-index or some local extreme index at a predefined lead time, as opposed to the earlier mentioned rolling climate predictions, who propagate the whole atmosphere for as many timesteps as desired (Bracco et al. (2025) and references therein). Their predictions have often proven more accurate than forecasts based on dynamical climate model output. The difference to the more modest postprocessing methods we are considering in this study is their tracing the whole causal chain outlined above from the initial boundary conditions to the surface parameters in one single model, i.e. black box. So in one way or another, sophisticated statistics can indeed make the difference, when it comes to producing decision-relevant climate forecasts.

In Sec. 2 we will present our dataset along with a remark on detrending. The PLS is outlined in Sec. 3. Its implementation along with some postprocessing applications are explained and their results discussed in Sec. 4. Sec. 5 draws the final conclusions.

2 Data

This study constructs targeted teleconnections on the basis of MSLP, T2M and PR seasonally averaged data from the ECMWF's reanalysis ERA5 (Hersbach et al., 2020) in the period 1951–2020. The MSLP patterns are calculated over the NAE sector $[-90, 60]^\circ$ E $\times$ $[20, 85]^\circ$ N. Goutham et al. (2023) Sec. 5.a discusses the choice of the domain, its size and location covering the whole North Atlantic upstream of Europe in detail. The target data consists of T2M and PR on the territory of Germany, but any other variable in any other region from any other observational data set would do.

The teleconnections are later on applied to postprocess the seasonal hindcasts produced with the global seasonal prediction model GCFS2.1 (Baehr et al., 2015). The hindcasts cover the period from 1990 to 2020 and consist of 30 ensemble members per initialization date (1st of each month) and are propagated for six months. The ERA5 data is regridded to the native grid of GCFS2.1 with grid size approximately 1°.

2.1 Note on Detrending

The statistical method we are going to use, PLS, is based on covariance. Covariance estimators are prone to trends in the data. When trends are present, they may show spurious covariance, even if there is non. Climate data, in turn, are very suspicious of containing trends due to global warming, depending on the parameter considered. It is therefore of utmost importance to remove trends that are external to circulation, i.e. thermodynamical trends. On the other hand, we want to retain everything

https://doi.org/10.5194/egusphere-2025-3664
Preprint. Discussion started: 8 August 2025

that is related to circulation, including dynamical trends induced by changes of circulation. That means our detrending must neither be too sophisticated. We suggest to subtract a simple parametric or nonparametric estimate of warming trends from temperature related variables, but to leave precipitation unchanged. Pressure, and more so geopotential height, is a delicate candidate, because it does respond to changing temperature. However, our experiments showed only barely noticeable influence of detrending MSLP on our targeted teleconnections. So we leave MSLP also undetrended.

3 Methods

3.1 Partial Least Squares Regression

As PLS is a well established dimension reduction technique with an host of existing very pedagogical literature, our presentation of PLS is going to draw heavily on one of them, which we deem exceptionally clear and intelligible. Rosipal and Krämer (2006):

> "In its general form PLS creates orthogonal score vectors (also called latent vectors or components) by maximizing the covariance between different sets of variables ... The predictor and predicted (response) variables are each considered as a block of variables. PLS then extracts the score vectors which serve as a new predictor representation and regresses the response variables on these new predictors."

Let $X \in \mathbb{R}^I$ and $Y \in \mathbb{R}^J$ two multivariate Gaussian random variables with mean 0, assumed to be related by linear regression, with I and J possibly very large, of which we observe n data samples. The predictor matrix $\mathrm{X} \in \mathbb{R}^{n \times I}$ and the response matrix $\mathrm{Y} \in \mathbb{R}^{n \times J}$ are decomposed into the form

$$\mathrm{X} = \mathrm{TP}^T + \mathrm{E} \qquad \mathrm{Y} = \mathrm{UQ}^T + \mathrm{F} \tag{1}$$

where $\mathrm{T} \in \mathbb{R}^{n \times k}$ and $\mathrm{U} \in \mathbb{R}^{n \times k}$ are the matrices of the k orthonormal score vectors (components, latent vectors), $\mathrm{P} \in \mathbb{R}^{I \times k}$ and $\mathrm{Q} \in \mathbb{R}^{J \times k}$ represent the loadings and $\mathrm{E} \in \mathbb{R}^{n \times I}$ and $\mathrm{F} \in \mathbb{R}^{n \times J}$ are the residuals.

The PLS method finds weight vectors w and v such that the resulting components t are maximally predictive for u:

$$\mathrm{cov}(t,u)^2 = \mathrm{cov}(Xw, Yv)^2 = \max_{|r|=|s|=1} \mathrm{cov}(Xr, Ys)^2 \tag{2}$$

where $\mathrm{cov}(t,u) = t^T u/n$ denotes the sample covariance.

The classical PLS method was originally defined by means of the nonlinear iterative partial least squares (NIPALS) algorithm (Wold, 1975). Høsskuldson (1988) later showed that w is the dominant eigenvector of $\mathrm{X}^T\mathrm{YY}^T\mathrm{X}$. Afterwards, Høsskuldson's algorithm proceeds analogously to NIPALS:

$$t = \mathrm{X}w \qquad v = \mathrm{Y}^T/t^T t \qquad u = \mathrm{Y}v \tag{3}$$

The first eigenvalue corresponds to the squared covariance between t and u. Using equations (1), the vectors of loadings p and q are computed as the regression coefficients of X on t and Y on u, respectively

$$p = \mathrm{X}^T t/(t^T t) \qquad q = \mathrm{Y}^T u/(u^T u) \tag{4}$$

https://doi.org/10.5194/egusphere-2025-3664
Preprint. Discussion started: 8 August 2025

The matrices X and Y are subsequently deflated by subtracting their rank-one approximations based on the scores. In PLS regression (PLS1/PLS2 as opposed to PLS mode A) the deflation of Y is carried out by the regression of Y on the predictor score t (rather than u).

$$\mathrm{X} = \mathrm{X} - tp^T \qquad \mathrm{Y} = \mathrm{Y} - tv^T \tag{5}$$

After deflation, the following pair of scores is extracted, and so on until a satisfactory result is achieved. This deflation scheme guarantees mutual orthogonality of the extracted score vectors $\{t_i\}_{i=1}^{p}$. It is indeed sufficient to deflate only one of the blocks (Dayal and MacGregor, 1997), or to deflate the covariance matrix directly leaving the X and Y blocks unaltered (De Jong, 1993).

Because of its special construction, PLS is often the method of choice when the X (and possibly the Y) data is highly co-linear and ordinary least squares (OLS) regression breakes down, as in the so-called $p > n$ *problem*, where more variables than samples are observed. Rosipal and Krämer (2006) (references therein):

> "PLS has been related to other regression methods like principal Component Regression (PCR) [26] and Ridge Regression (RR) [16] and all these methods can be cast under a unifying approach called continuum regression [40, 9]. The effectiveness of PLS has been studied theoretically in terms of its variance [32] and its shrinkage properties [12, 21, 7]. The performance of PLS is investigated in several simulation studies [11, 1]."

3.2 Related Methods

There exists a great number of PCA-related decomposition methods, which all project the original variables in one form or another to certain latent variables. Besides PCA itself, Canonical Correlation Analysis (CCA), PSL, Maximum Covariance Analysis (MCA), and RDA all belong to this category. We quote again from Rosipal and Krämer (2006):

> "The connections between PCA, CCA and PLS can be seen through the optimization criterion they use to define projection directions. PCA projects the original variables onto a direction of maximal variance called principal direction. Following the notation of (2), the optimization criterion of PCA can be written as
>
> $$\max_{|r|=1} \mathrm{var}(Xr)$$
>
> where $\mathrm{var}(t) = t^T t/n$ denotes the sample variance. Similarly, CCA finds the direction of maximal correlation solving the following optimization problem
>
> $$\max_{|r|=|s|=1} \mathrm{corr}(Xr, Ys)^2$$
>
> where $\mathrm{corr}(t,u)^2 = \mathrm{cov}(t,u)^2/\mathrm{var}(t)/\mathrm{var}(u)$ denotes the sample squared correlation. It is easy to see that the PLS criterion (2)
>
> $$\max_{|r|=|s|=1} \mathrm{cov}(Xr, Ys)^2 = \max_{|r|=|s|=1} \mathrm{var}(Xr)\mathrm{corr}(Xr, Ys)^2\mathrm{var}(Ys)$$

https://doi.org/10.5194/egusphere-2025-3664
Preprint. Discussion started: 8 August 2025

represents a form of CCA where the criterion of maximal correlation is balanced with the requirement to explain as much variance as possible in both X- and Y-spaces."

The last two projection methods that we want to mention here are MCA and RDA. MCA maximizes the same optimization criterion as PLS. But whereas PLS retrieves the latent variables sequentially from alternately deflated X and Y variables, MCA retrieves them all simultaneously from the SVD of the original covariance matrix $\mathrm{X}^T\mathrm{Y}$. This procedure is symmetric like CCA and results in a different decomposition, slightly less efficient in terms of regression. Rosipal and Krämer (2006) discusses MCA under the name of PLS-SB as a variant of PLS.

In constrast, RDA (Goutham et al., 2023) works similarly to MCA, but the predictor variables are asymmetrically whitend/-sphered before taking the covariance. The sphering of X entails the inversion of the covariance matrix of X: $\mathrm{X}' = (\mathrm{X}^T\mathrm{X})^{-1/2}\mathrm{X}$. If the covariance matrix of X is close to singular, the inversion of $\mathrm{X}^T\mathrm{X}$ becomes a delicate matter. This problem occurs when heavy co-linearities exist in the X data as is necessarily the case for $p > n$—the very reason why we need to replace the OLS in the first place. RDA is therefore not our method of choice. Although not mentioned in Rosipal and Krämer (2006), the same problem befalls CCA in the calculation of the correlation matrix, so that CCA is usually applied only after a preliminary truncated PCA.

4 Applications

Let us note that the targeted teleconnections-algorithm is applicable to all kinds of predictor and target fields comprising scalar (PLS1), vector (PLS2), matrix, and tensor-valued (N-PLS (Bro, 1996)) time series, as long as, apart from having an approximately linear relationship, the random variables are at least roughly Gaussian, i.e. have a finite variance and are more or less symmetric, such that the Least Squares Estimator≈Maximum Likelihood Estimator. Non-Gaussian variables with a continuous density could be converted to Gaussian ones by a distribution transform, while the minimization criterion would be distorted likewise. In contrast, this is not possible for distributions with point-mass on particular values like daily PR or some of the various climate indicators, which are very much in use today. There exist many specific variants of PLS for these and other deviations from the assumptions of classical PLS.

- Discrete targets: PLS for classification and discrimination
- Contaminated targets: robust weighted PLS where both outliers and leverage points are iteratively weighted down
- Non-Gaussian (skewed, heavy-tailed ...) targets: Partial Least Distance Squares (PLDS) substituting distance covariance for product covariance, PLS combined with Independent Component Analysis (IDA)
- Non-linear relationships between predictor and target: Kernel-PLS is by far the most successful approach.

The discussion of those variants is beyond the scope of this study.

https://doi.org/10.5194/egusphere-2025-3664
Preprint. Discussion started: 8 August 2025

4.1 Teleconnections targeted at 2 meter temperature in Germany

Here, we will give a detailed description of how to construct targeted teleconnections to maximize explanatory power for temperature in Germany on the seasonal timescale. Our ultimate goal is to postprocess seasonal forecasts of DWD's GCFS2.1, which predicts seasonal averages with lead times of 0 to 3 months (e.g. a forecast initialized January, 1st predicts 3-monthly means or JFM, FMA, MAM and AMJ). So we take the time series of seasonal averages of ERA5 MSLP and T2M (JFM, FMA, MAM...) to describe interannual variability and covariability of seasonal circulation and temperature. But the same computations are evidently also possible on any other time scale, on which traditional EOF teleconnections are usually derived.

Firstly, we check that the Gaussianity assumption is sufficiently well fulfilled for both seasonal MSLP and T2M anomalies. As discussed in Sec. 2, we apply a simple detrending to T2M only, by calculating an overall trend of the spatial average over the territory of Germany and subtracting it from the individual grid cell time series. To ensure generality, we conduct the same experiment with two different forms of trend: i) a quadratic trend to allow for increased warming towards the end of the time period, which seems very appropriate for a temperature time series starting in 1950; ii) a trend of lagging 15-year averages so as to extend the advantage of having a nonparametric trend right through 2020 as applied in Goutham et al. (2023). We found no visible difference in the results caused by the two forms of detrending. The MSLP anomalies are calculated without detrending. An area weighting of $\sqrt{\cos(lat)}$ is applied.

For numerical reasons, we rescale the whole seasonal fields of MSLP and T2M by their square root sums of squares (Frobenius norm). After the procedure, the component patterns are remultiplied by those factors to bring them back to their physical units. Additionally, we standardize the index time series by their standard deviation and also multiply it to the patterns.

We are now in a position to feed our pairs of blocks of predictor and response variables into the PLS algorithm[1], one season at a time. Let us repeat our warning that the targeted teleconnections must not be mistaken for variability modes of the circulation. They are in contrast the modes of covariability, which exert the strongest influence from the circulation onto the target.

To begin with, we have a look at the correlations between the newly produced targeted teleconnection indices and the target, i.e. T2M in Germany. Table 1 gives the average coefficients of determination achieved by regressing each grid cell's T2M time series on the two principle indices in the four main seasons. The indices derived by EOF and those derived by PLS for both MSLP, the actual teleconnections, and for T2M, the target, are contrasted. We decided to regress T2M on only two teleconnections, because when dealing with indices estimated from samples (either dynamical climate model output or observations) the trailing indices are less robust. And the trade-off between additional explanatory power and estimation uncertainty quickly tilts to the negative.

We appreciate that the target indices explain the T2M values very closely, though slightly less so in summer. We further appreciate that the coefficients of determination are always higher in the PLS teleconnections than in the EOF teleconnections. But we notice that in winter the untargeted EOF indices explain nearly as much of the T2M variation in Germany as the targeted indices. This is surely one reason, why large part of the studies involving the impact of EOF teleconnections on surface climate

[1] We deflate the covariance matrix directly according to De Jong (1993).

https://doi.org/10.5194/egusphere-2025-3664
Preprint. Discussion started: 8 August 2025

Table 1. average coefficients of determination for ERA5 T2M and PR in Germany using two teleconnections

	EOF(MSLP)	PLS(MSLP|target)	PLS(target)
T2M Germany			
DJF	0.7798	0.8217	0.8937
MAM	0.5428	0.6658	0.8087
JJA	0.3529	0.6063	0.7075
SON	0.3829	0.6393	0.8497
PR Germany			
DJF	0.2916	0.6373	0.8583
MAM	0.2919	0.6652	0.8173
JJA	0.3716	0.5588	0.7840
SON	0.4107	0.6502	0.8338

in Europe focus on the winter season. Lastly we observe that this relation changes for the other seasons. There, the transition from EOF to PLS teleconnections entails a substantial gain in explanatory power.

We now have a look on the corresponding circulation and target patterns. Fig. 1 shows the two dominant patterns for each of the main seasons. As the coefficients of determination already hinted to, in winter the EOF and PLS patterns of MSLP are very similar. NAO and EA are clearly recognizable, with the southern center of action of NAO in the PLS pattern slightly weaker than in der EOF pattern. Both positive anomalies of NAO and EA in the PLS patterns are shifted eastwards, which seems plausible given the location of the target region. The respective T2M patterns correspond to the well-known impact of these teleconnections on European T2M (Simpson et al., 2024).

The differences are more pronounced in the other seasons, with the second patterns in spring and summer and both patterns in autumn being very different. Although a comparison of our winter PLS teleconnections to those of Goutham et al. (2023) is rather hampered by different settings (MSLP vs. ZG500, seasonal vs. weekly time scale, target domains Germany vs. Europe+surrounding seas), the patterns are reasonably similar, and Goutham et al. (2023)'s detailed discussion of the differences between their RDA patterns and the traditional EOF patterns in their Sec. 4.a applies in large part also to our PLS patterns. We notice further that our T2M patterns are only slightly structured owing to the small target domain and the smooth response of temperature to circulation patterns.

Analogously constructed teleconnection patterns targeted to PR seasonal sums over Germany can be found in the Supporting Information Fig. S1.

4.2 North–Atlantic European Ocean–Atmosphere Interactions

As already noted above, the targeted teleconnections algorithm based on PLS is a very versatile tool. Ultimately, a number of studies have been published about the interaction between the NAE circulation with the underlying ocean in the framework of decadal climate predictions (Patrizio et al., 2025; Kolstad and O'Reilly, 2024; Patterson et al., 2024). Some of these studies

https://doi.org/10.5194/egusphere-2025-3664
Preprint. Discussion started: 8 August 2025

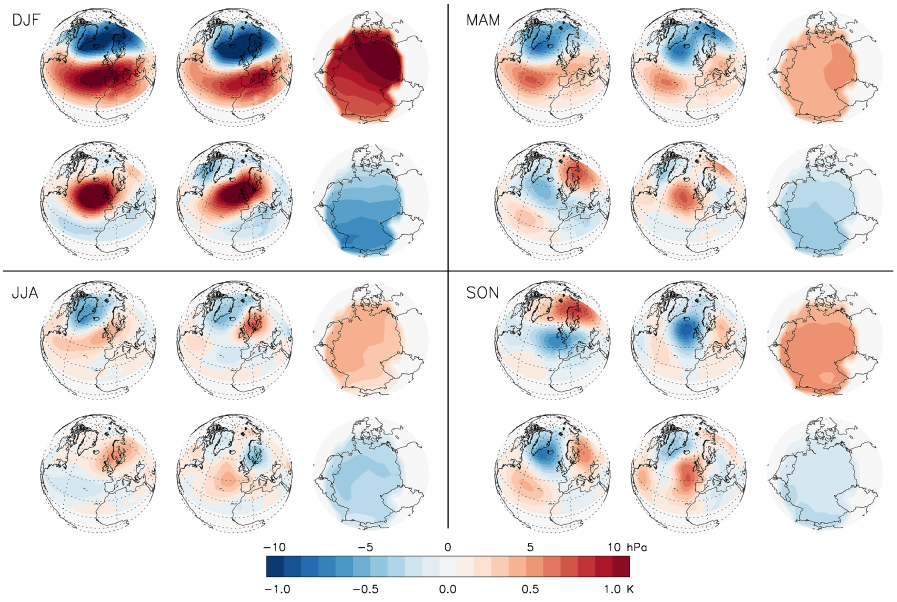

Figure 1. NAE seasonal teleconnection patterns. Seasonal subplots left/center/right colums: untargeted MSLP (EOF)/T2M-targeted MSLP/respective T2M-patterns. Upper/lower rows: first/second dominant patterns.

are using rather complicated methodologies in the attempt to pin down the causal impact of sea surface temperatures (SST) onto the circulation. We suggest that an analysis of targeted teleconnections from SST to MSLP could be very helpful in this context, as it finds those predictor and target coupled modes of variability, which maximize predictability (Fig. 2).

Comparing Fig. 3 of Patrizio et al. (2025), Fig. 6 of Patterson et al. (2024) and Fig. 1 of Kolstad and O'Reilly (2024) to our Fig. 2 (DJF), we find the same well-known oceanic tri-pole pattern associated with the NAO di-pole, and furthermore in Patterson et al. (2024) also the large anomaly in the central NA connected to an EA-like mono-pole over the North Atlantic. The patterns in the other seasons are resembling variations of the same theme.

When the PLS algorithm is applied to SSTs lagging MSLP, then the relationship can be exploited to statistically predict the future atmospheric circulation from observed SSTs. DWD's empirical first guess MSLP indices used in ensemble subsampling are actually based on this idea (see Sec. 4.3.1).

4.3 Postprocessing Applications

The following examplary applications to dynamical model output are meant to highlight the possible gains that can be achieved by substituting targeted teleconnection for untargeted ones. They should be understood as a proof of concept, not an exhaustive list.

https://doi.org/10.5194/egusphere-2025-3664
Preprint. Discussion started: 8 August 2025

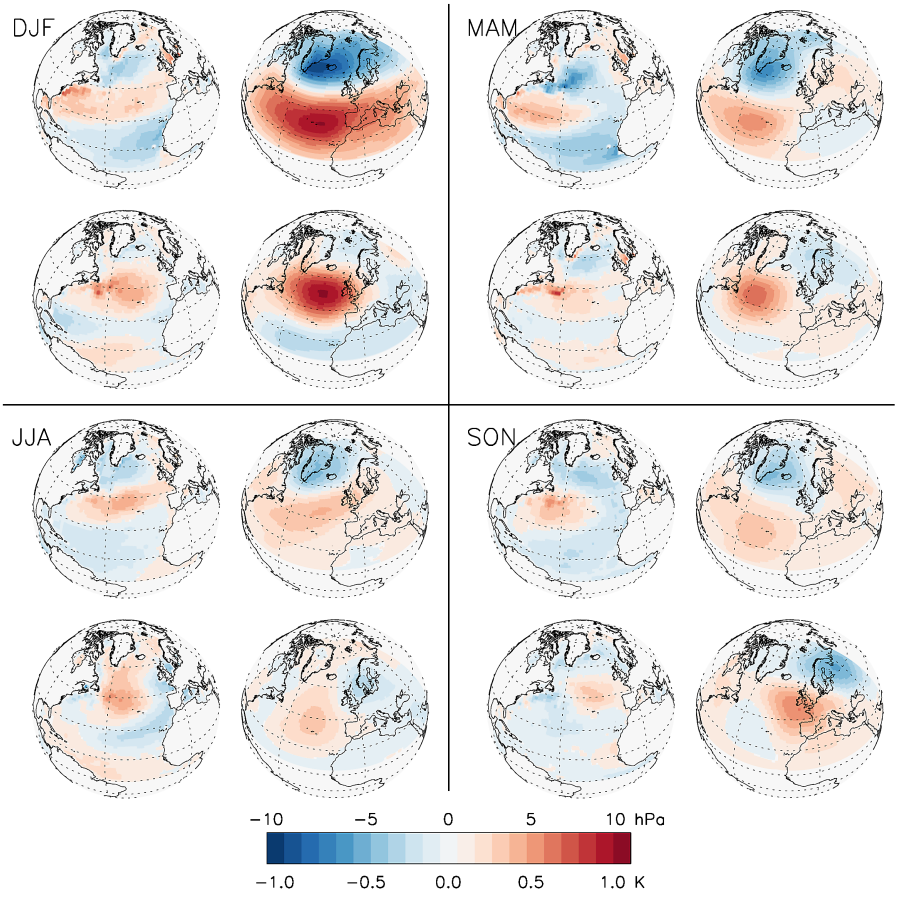

Figure 2. Seasonal NAE ocean–atmosphere interaction patterns. Seasonal subplots left/right colums: MSLP-targeted SST/respective MSLP-patterns. Upper/lower rows: first/second dominant patterns.

4.3.1 Ensemble Subsampling

In DWD, seasonal forecasts of GCFS2.1 with initialization dates from September to December are postprocessed with a subsampling algorithm, which selects forecast ensemble members according to their closeness to an empirical first guess of the future circulation indices. Fig. 3 row (a) shows the mean squared error skill scores (MSESS) of the seasonal ensemble mean hindcasts initialized in September for T2M wrt. climatology for lead times 0 to 3 months with rather modest skill. Rows (b) and (c) show subselected hindcasts, where the true (EOF and PLS, respectively) teleconnection indices are applied. We chose to showcase the hindcast initialized on September 1, because it covers both the SON and the DJF season, which present opposite behaviors in their coefficients of determination as listed in Table 1. The subsampling applied to true indices marks the limits to the potential improvement, when estimation errors are zero. Whilest the subsampled hindcast for DJF wrt. untargeted telecconections is equally skillful as the one subsampled wrt. T2M-targeted teleconnections, the other hindcasts'

https://doi.org/10.5194/egusphere-2025-3664
Preprint. Discussion started: 8 August 2025

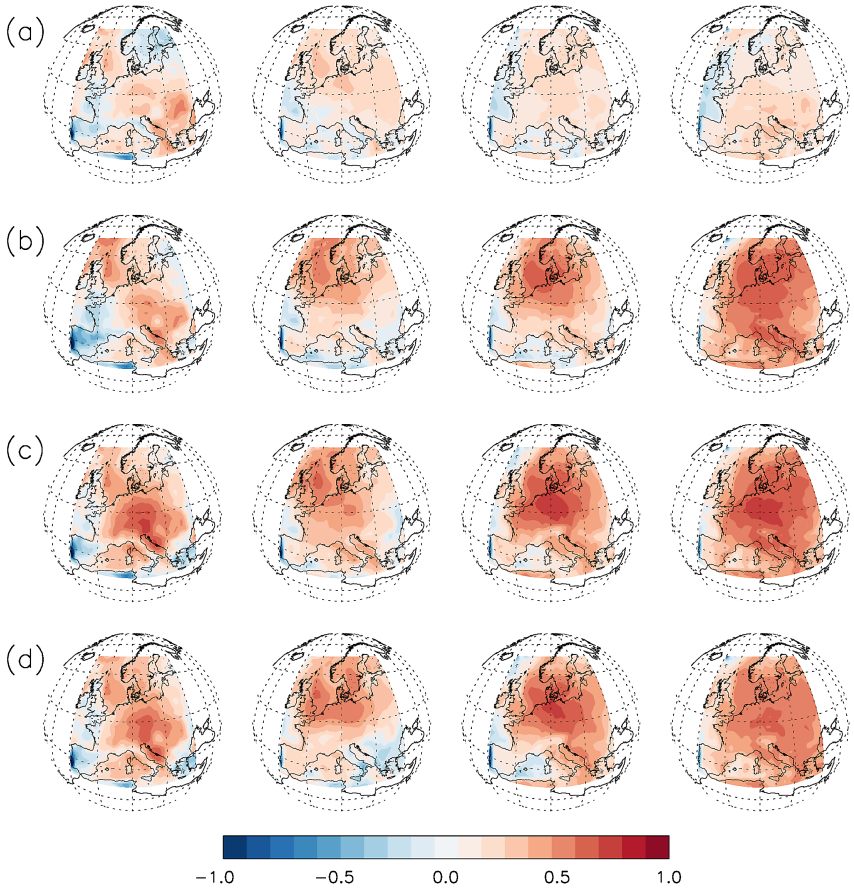

Figure 3. MSESS of seasonal T2M GCFS2.1 hindcasts initialized in September. (a) ensemble mean; (b) subensemble mean based on true untargeted teleconnctions; (c) subensemble mean based on true T2M-targeted teleconnections; (d) subensemble mean based on empirically predicted T2M-targeted teleconnections. Left to right: lead times SON to DJF.

skill does indeed improve. (Not shown: anomaly correlation coefficients (ACC) are substancially improved, ranked probability skill scores (RPSS) only slightly so due to very low subsampled ensemble size around 10 members, but are nevertheless nearly everywhere positive in contrast to the full ensemble mean.)

When plugging in DWD's actual empirical first guess produced with advanced machine learning techniques[2] for the targeted teleconnection indices (Fig. 3 (d)), the result falls only slightly short of the optimum. (Analogous plots for all start months in the Supporting Information S2 to S13.)

[2]Tensor PLS regression of the selected circulation index onto the 3-modal tensor of the latest 6 months of sea surface temperature (SST).

https://doi.org/10.5194/egusphere-2025-3664
Preprint. Discussion started: 8 August 2025

Table 2. correlation coefficients of the dominant untargeted/targeted teleconnection indices of the forecast ensemble mean initialized in December and subensemble mean selected wrt. T2M-targeted teleconnections of GCFS2.1 against ERA5

lead	EOF_{EM}(MSLP)	EOF_{sub}(MSLP)	PLS_{sub}(MSLP|T2M)	PLS_{sub}(MSLP|PR)
0	0.514	0.842	0.828	0.772
1	0.068	0.742	0.753	0.705
2	0.024	0.779	0.759	0.529
3	0.014	0.785	0.774	0.720

4.3.2 Statistical Downscaling

The other major application of teleconnections in postprocessing is statistical downscaling, where the observational relationship between the circulation and the surface parameters is transferred to the large scale climate model output. Namely, the model produced circulation indices are multiplied with the target patterns and superposed to form the prediction. This can be done either at individual hindcast member level or at ensemble mean level, ultimately leading to the same prediction due to linearity.

In Fig. 4, we show the improvement in MSESS that can be achieved by the use of targeted teleconnections as compared to traditional ones, given the large scale circulation model output is reasonably skillful. This time GCFS2.1 hindcasts initialized on December 1 for PR are presented. Row (a) again shows the ensemble mean hindcasts, which have mostly negative skill except at lead time 0. Row (b) shows the skill, when the ensemble mean MSLP hindcast is downscaled based on the EOF teleconnection indices with their respective PR-projections. The MSESS thereby increases to levels around zero, but nothing more.

In search of an explanation for the low skill, we have a look at the correlation of the dominant teleconnection indices that are predicted by GCFS2.1 wrt. ERA5 (Table 2). At lead time 0 the ensemble mean dominant EOF index (column 2) reaches a respectable correlation to ERA5 of > 0.5, similarly the ensemble mean PR prediction at lead 0 is quite good (being PR). At later lead times the correlation between ensemble mean and ERA5 indices drops off dramatically to zero. But the skill of the PR hindcast becomes even negative (Fig. 4 row (a)), despite the correlation of the teleconnection indices being not. This can only mean that the teleconnection between circulation and PR is not well represented by the model. It is therefore consistent that downscaling improves the MSESS, but only so much as predetermined by the MSLP field.

If we were able to find a more skillful hindcast for the teleconnection index, it is not impossible that the skill of the downscaled PR might increase as well. Having constructed hindcasts with improved circulation representation by means of subsampling, we take those as our obvious candidates. Table 2 corroborates that the subsampling (despite being targeted at T2M) improves not only the T2M-targeted teleconnection indices (column 4), but also the untargeted ones (column 3) and even those targeted at PR (column 5). This should not come as a surprise given that all circulation indices live on the same MSLP fields. But caution, the connection is not always strong, depending on the season.

When downscaling the subensemble mean using untargeted EOF teleconnections, the MSESS shows still the same patchy pattern as for the downscaled full ensemble mean with very low MSESS covering about the half of the domain against 0 in the

https://doi.org/10.5194/egusphere-2025-3664
Preprint. Discussion started: 8 August 2025

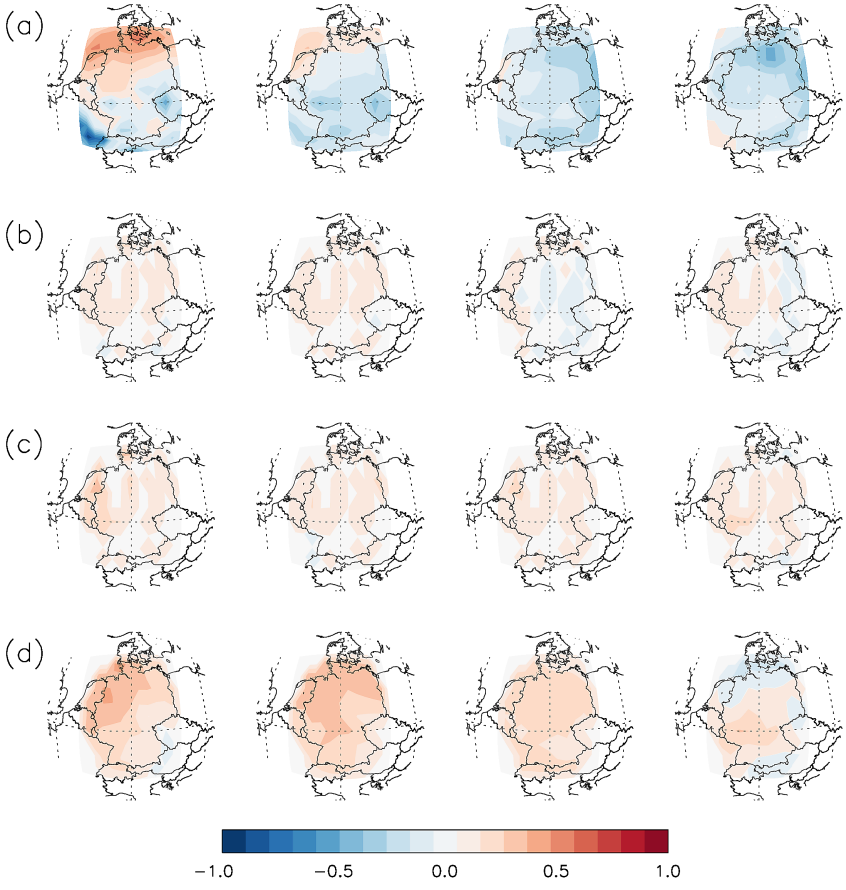

Figure 4. MSESS of seasonal PR GFCS2.1 hindcasts initialized in December. (a) ensemble mean; (b) ensemble mean downscaled with EOF teleconnctions; (c) subensemble mean based on empirical prediction of T2M-targeted teleconnections, downscaled with untargeted teleconnections; (d) subensemble mean based on empirical prediction of T2M-targetd teleconnections, downscaled with PR-targeted teleconnections. Left to right: lead times DJF to MAM.

other half, only this time the slightly negative values have turned positive (Fig. 4 row (c)). This is caused by the low coefficients of determination from the EOF indices to PR (Table 1). To take advantage of their much higher coefficients of determination, we replace the EOF teleconnections by their PR-targeted counterparts (evidently, we can project the model output MSLP fields on as many circulation patterns as we please). This time we get a modest, yet nearly uniformly positive MSESS (Fig. 4 row (d)). (Analogous plots for all start months in the Supporting Information S14 to S25.)

Of course, we could have subsampled the ensemble wrt. an empirical estimate of the PR-targeted teleconnections in the first place. However, the poor representation of the MSLP–PR relationship in GCFS impedes a substantial improvement of the subensemble PR hindcasts, while lowering the skill of T2M. On the other hand, the two independently subsampled hindcasts, T2M subsampled wrt. T2M and PR subsampled wrt. PR, would not be consistent with each other, because they are most proba-

https://doi.org/10.5194/egusphere-2025-3664
Preprint. Discussion started: 8 August 2025

Table 3. mean of MSESS over all initialization dates, lead times, and grid cells in the target region for various subsampling/downscaling strategies

	$\text{MSESS}(\text{T2M}_{\text{sub}})$	$\text{MSESS}(\text{PR}_{\text{sub}})$	$\text{MSESS}(\text{PR}_{\text{sub+down}})$
T2M-targeted	0.338	-0.054	0.062
PR-targeted	0.143	0.055	0.156
T2M+PR-targeted	0.321	-0.015	0.135

bly based on different ensemble members. In contrast, T2M subsampled wrt. T2M and PR subsampled wrt. T2M+downscaled wrt. PR are indeed consistent due to the shared MSLP fields. A further experiment to subsample wrt. T2M-targeted and PR-targeted teleconnection indices at the same time proved worthwhile in giving nearly the same MSESSs for T2M and PR as the respective single-field-targeted subensembles (Table 3).

4.3.3 Multimodel Ensemble Weighting

Ensemble weighting (Sánchez-García et al., 2019) is a general postprocessing approach that encompasses subsampling, in the sense that subsampling is a 0/1-weighting. It also enables a more accurate estimation of key winter circulation features, specifically the NAO, which is strongly linked to temperature and precipitation anomalies across much of Europe and the Mediterranean. Ensemble weighting reduces or eliminates the originally equal weight of those ensemble members, which poorly represent a given NAO forecast, which is supposed to be more accurate than the forecast ensemble mean.

The possibility to extend this technique to incorporate other NAE variability modes in an application to T2M and PR forecasts over the Iberian Peninsula is explored next. Note that our ability to improve the forecast of a target variable is influenced by two factors: on one hand, the amount of variance of the target variable that can be explained by the variability mode, and, on the other hand, our ability to predict the mode accurately, so we can weight the ensemble accordingly. In (Sánchez-García et al., 2019), both preconditions are fulfilled: NAO shows a strong correlation with winter precipitation over the Iberian Peninsula, and an empirical model which skillfully predicts NAO was developed.

In order to evaluate whether incorporating additional variability patterns beyond the NAO can improve the predictive value, and to assess this technique's potential through other seasons, the first four EOFs of the seasonal MSLP anomalies are computed over the NAE sector (90°W–60°E, 20°–85°N), which will be used as our variability patterns. The observed phase $(\text{PC}_k^*)_{k=1}^4$ of the modes according to ERA5 is used as an idealized "perfect" prediction for each hindcast year. Ensemble members are weighted such that more weight is assigned to members i with a phase vector $(\text{PC}_{ik})_{k=1}^4$ similar to that of the "perfect" prediction, using a weight function based on the **Cauchy kernel** defined as

$$w_i(h) \;=\; \frac{1}{1+\left(\frac{1}{h}\sum_{k=1}^{K} v_k \cdot |\text{PC}_{ik}-\text{PC}_k^*|\right)^2}$$

where v_k is the eigenvalue of the k-th mode (normalized so that $\sum_k v_k = 1$), and $K = 4$ is the number of modes used, and the bandwidth parameter $h = 1$.

https://doi.org/10.5194/egusphere-2025-3664
Preprint. Discussion started: 8 August 2025

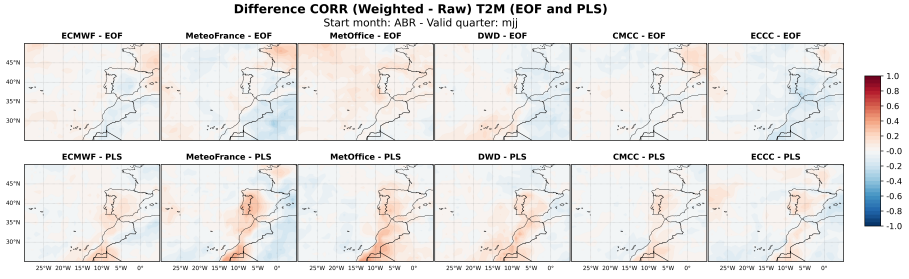

Figure 5. Difference in Spearman correlation between observed and weighted/unweighted hindcast anomalies (start date April) for T2M averaged over MJJ in six C3S seasonal forecast models. upper row: weighting wrt. EOF modes; lower row: weighting wrt. PLS modes

Weighting the ensemble using NAE variability modes leads to an improvement of the forecast for T2M and PR in winter–early spring, whereas a slight improvement is observed from April–May to October (Supporting Information Fig. S26 and S27). This seasonal contrast may be related to the EOF modes capturing a higher fraction of T2M and PR variance in Iberia over the winter months.

This raises the question whether an alternative definition of the modes used for ensemble weighting could improve forecast skill in those months, which do not profit from weighting with EOF modes, such as April–October.

To assess whether an alternative basis for the modes could lead to further improvement in the warm season, we construct targeted teleconnection indices using the PLS methodology described in Sec. 3.

The predictor is once again MSLP anomalies over the NAO sector, while the predictands are T2M and PR anomalies over Iberia. The modes are obtained using the PLS regression implementation from the scikit-learn Python library.

For direct comparison, we calculate the first four modes, and apply the same methodology as for the EOF modes (Supporting Information Fig. S28 and S29). When doing so, we find no improvement against EOF for October–March months, neither for T2M nor PR. However, for this period, EOF-computed modes already explain a significant amount of variance, so it is not straightforward to find an improvement by changing the definition of the modes. In contrast, comparing T2M results from the AMJ to JJA seasons and for ASO, a gain in forecast skill is observed when using PLS-based modes. In the spatial maps of Spearman correlation difference between weighted/unweighted T2M ensemble hindcasts initialised in April with lead time MJJ, most of Iberia experiences an improvement in skill (Fig. 5).

PR, however, does not show a clear improvement over Iberia during spring–autumn. The limited skill improvement may be linked to the convective nature of precipitation in spring and summer in Iberia, with precipitation being highly dependent on local fluxes and humidity advection, and less so on the mean circulation, as opposed to winter.

Additional tests suggest that more potential for improvement can be found using different weighting functions and bandwidths. A variation in the number of modes (1–4) is equally worth studying, as there could be a risk of introducing some over-fitting with too many modes.

https://doi.org/10.5194/egusphere-2025-3664
Preprint. Discussion started: 8 August 2025

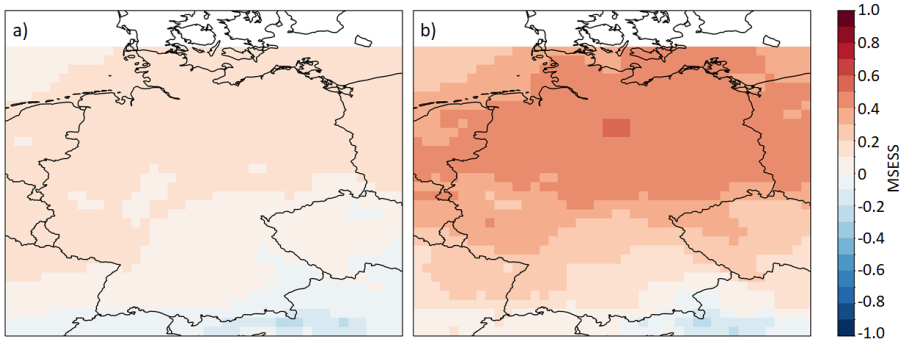

Figure 6. MSESS of seasonal 100m wind speed GFCS2.1 hindcasts initialized in November for leadtime DJF. left: ensemble mean; right: subensemble mean based on empirically predicted T2M-targeted teleconnections.

Our preliminary results provide evidence that the use of targeted variability modes can offer an opportunity to improve seasonal forecasts in Iberia in line with what has been shown for Germany and have the potential to enhance ensemble weighting approaches beyond the winter season in the majority of the models.

Of course, the skill of predicting the modes still remains to be assessed: we may have modes that explain a high amount of variability of the target variables, but we also need to be able to predict them to fulfill this potential. Future work will try to refine the methodology for Iberia and explore the ability of the models to predict the targeted teleconnection modes.

4.3.4 Wind, Solar and Energy Forecasts Based on a Subensemble

Forecasts for energy related variables like 100m wind speed and solar radiation, as well as the forecast of renewable energy production is challenging on seasonal timescales (Lledó et al., 2019; Bett et al., 2022; Tyagi et al., 2025b). Substantial skill only emerges in selected months (i.e. DJF for 100m wind speed and energy and JAS for solar radiation (not shown)). Therefore given the growing need for accurate seasonal forecasts for the energy sector (Orlov et al., 2020), we apply the subensemble based on empirically predicted T2M-targeted teleconnections to seasonal GCFS2.1 hindcasts (1991–2020) of 100m wind speed, solar radiation and renewable energy production.

For 100m wind speed and solar radiation, we see an improvement in skill (measured by MSESS, ACC and RPSS) compared to the full ensemble for most of the tested initialization dates (February, Mai, August, November) and lead times (0 to 3 months). The improvement is especially pronounced for 100m wind speed hindcasts initialized in November (Fig. 6) and May (not shown) and for solar radiation hindcasts initialized in February and May (not shown). Moreover, for 100m wind speed hindcasts initialized in November the subensemble based on T2M-targeted teleconnections performs better than the current operational version of the subsampling (Dalelane et al., 2020) based on traditional EOFs. Still, some initialization dates and specific lead times show less to no improvement in skill compared to the full ensemble or the current operational subsampling (not shown). In conclusion, the results indicate that T2M-targeted teleconnections can also yield an added value to seasonal forecasts of other variables like 100m wind speed and solar radiation.

https://doi.org/10.5194/egusphere-2025-3664
Preprint. Discussion started: 8 August 2025

Seasonal wind energy forecasts derived from a physical model using 10 m wind speeds exhibit similar patterns of skill improvement based on the same subensemble as those based on 100 m wind speeds. Notably, a substantial increase in predictive skill is observed across all lead times for forecasts targeting the extended winter period (November to February). Interestingly, this season also coincides with the highest variability in wind energy production. The overlap between enhanced forecast skill and peak variability presents promising opportunities for the wind energy sector (Tyagi et al., 2025a).

5 Summary

In this study, we have proposed targeted teleconnections as a means to construct circulation indices that are maximally predictive for a chosen target variable in the sense of linear regression. We have shown its application to T2M gridded fields over Germany from ERA5, highlighting their increased potential to predict this target in comparison to traditional circulation indices (NAO, EA ...). Their subsequent use in the subsampling and downscaling of dynamical model output has elicited promising results, such that their implementation will allow the DWD to provide to the public subsampled seasonal forecasts of temperature and precipitation with strongly improved forecast skill as of autumn 2025 (see specific climate predictions on www.dwd.de/climatepredictions).

It was further shown that due to strong correlation with T2M, the skill of the subsampled seasonal forecasts also carries over to derived seasonal forecasts for 100m windspeed, solar radiation and renewable energy production.

The PLS methodology was successfully transferred to the Iberian Peninsula and the derived targeted teleconnection modes implemented into an ensemble weighting procedure.

Similar to the targeted teleconnections between MSLP and T2M/PR, coupled modes of the NAE ocean–atmosphere interaction were calculated between SST and MSLP, which could be of potential use in decadal climate prediction.

Let us emphasize that the technical implementation of targeted teleconnections to user-selected climate fields is relatively easy given the standard provision of PLS algorithms in virtually all statistical software packages. Targeted teleconnections are adaptable to a wide range of climate variables, the only assumption being their approximate Gaussianity. Even for target variables violating this assumption, there are variants of PLS that can deal with classification and non-linear regression.

We would like to promote the consideration of using targeted teleconnections as an alternative to traditional EOF-based circulation indices in all applications, where the latter have proven beneficial, and including in situations, where a theoretical possibility exists, but has not worked out due to low correlation between EOF modes and targets.

Code and data availability. ERA5 data are available at https://cds.climate.copernicus.eu/. GCFS2.1 hindcasts are available at https://esgf-metagrid.cloud.dkrz.de/. Ready-to-use PLS implementations are available in virtually every statistical software distribution including open-source packages for R and Python.

https://doi.org/10.5194/egusphere-2025-3664
Preprint. Discussion started: 8 August 2025

Author contributions. **CD**: Conceptualization, Methodology, Investigation, Software, Visualization, Writing – original draft, review and editing. **MS, SS, ERG**: Sec. 4.3.3. **JW, AT**: Sec. 4.3.4. **AP**: Writing – review and editing

Competing interests. The authors declare that they have no known competing financial interests or personal relationships that could have appeared to influence the work reported in this paper.

Acknowledgements. We are thankful to our collegue Fabiana Castino, who's efforts to apply the proposed targeted teleconnections methodology to the heatwave magnitude index drew our attention to the importance of the Gaussian assumption on the target variables.

https://doi.org/10.5194/egusphere-2025-3664
Preprint. Discussion started: 8 August 2025

References

Baehr, J., Fröhlich, K., Botzet, M., and et al.: The prediction of surface temperature in the new seasonal prediction system based on the MPI-ESM coupled climate model, CLIM DYN, 44, 2723–2735, https://doi.org/10.1007/s00382-014-2399-7, 2015.

Baker, L. H., Shaffreya, L. C., and Scaife, A. A.: Improved seasonal prediction of UK regional precipitation using atmospheric circulation, INT J CLIMATOL, 38, e437–e453, https://doi.org/https://doi.org/10.1002/joc.5382, 2018.

Bednorz, E., Czernecki, B., Tomczyk, A. M., and Półrolniczak, M.: If not NAO then what?–regional circulation patterns governing summer air temperatures in Poland, THEOR APPL CLIMATOL, 136, 1325–1337, https://doi.org/10.1007/s00704-018-2562-x, 2019.

Benassi, M., Athanasiadis, P., Borrelli, A., Cavicchia, L., Gualdi, S., Hashemi Devin, M., Sanna, A., and Tibaldi, S.: A NAO-based subsampling approach for winter seasonal prediction, EMS Annual Meeting 2024, Barcelona, Spain, 1-6 Sep 2024, EMS2024-529, https://doi.org/10.5194/ems2024-529, 2024.

Bett, P. E., Thornton, H. E., Troccoli, A., De Felice, M., Suckling, E., Dubus, L., Saint-Drenan, Y.-M., and Brayshaw, D. J.: A simplified seasonal forecasting strategy, applied to wind and solar power in Europe, Climate Services, 27, 100 318, https://doi.org/https://doi.org/10.1016/j.cliser.2022.100318, 2022.

Bloomfield, H. C., Brayshaw, D. J., and Charlton-Perez, A. J.: Characterizing the winter meteorological drivers of the European electricity system using targeted circulation types, METEOROL APPL, 27(1), e1858, https://doi.org/10.1002/met.1858, 2020.

Bloomfield, H. C., Brayshaw, D. J., Gonzalez, P. L. M., and Charlton-Perez, A.: Pattern-based conditioning enhances sub-seasonal prediction skill of European national energy variables, METEOROL APPL, 28(4), e2018, https://doi.org/10.1002/met.2018, 2021.

Bracco, A., Brajard, J., Dijkstra, H. A., Hassanzadeh, P., Lessig, C., and Monteleoni, C.: Machine learning for the physics of climate, NAT REV PHYSICS, 7, 6–20, https://doi.org/10.1038/s42254-024-00776-3, 2025.

Bro, R.: Multiway calibration. Multilinear PLS, J CHEMOMETR, 10(1), 47–61, https://doi.org/10.1002/(SICI)1099-128X(199601)10:1<47::AID-CEM400>3.0.CO;2-C, 1996.

Cionni, I., Lledó, L., Torralba, V., and Dell'Aquila, A.: Seasonal predictions of energy-relevant climate variables through Euro-Atlantic teleconnections, Climate Services, 26, 100 294, https://doi.org/10.1016/j.cliser.2022.100294, 2022.

Dalelane, C., Dobrynin, M., and Fröhlich, K.: Seasonal Forecasts of Winter Temperature Improved by Higher-Order Modes of Mean Sea Level Pressure Variability in the North Atlantic Sector, GEOPHYS RES LETT, 47(16), e2020GL088 717, https://doi.org/10.1029/2020GL088717, 2020.

Dayal, B. S. and MacGregor, J. F.: Improved PLS algorithms, J CHEMOMETR, 11(1), 73–85, https://doi.org/10.1002/(SICI)1099-128X(199701)11:1<73::AID-CEM435>3.0.CO;2-%23, 1997.

De Jong, S.: SIMPLS: an alternative approach to partial least squares regression, CHEMOMETR INTELL LAB, 18(3), 251–263, https://doi.org/10.1016/0169-7439(93)85002-X, 1993.

Dobrynin, M., Domeisen, D. I. V., Müller, W. A., Bell, L., Brune, B., Bunzel, F., Düsterhus, A., Fröhlich, K., Pohlmann, H., and Baehr, J.: Improved Teleconnection-Based Dynamical Seasonal Predictions of Boreal Winter, GEOPHYS RES LETT, 45(8), 2723–2735, https://doi.org/10.1007/s00382-014-2399-7, 2018.

Dorrington, J., Finney, I., Palmer, T., and Weisheimer, A.: Beyond skill scores: exploring sub-seasonal forecast value through a case-study of French month-ahead energy prediction, Q J ROY METEOR SOC, 146(733), 3623–3637, https://doi.org/10.1002/qj.3863, 2020.

Faranda, D., Messori, G., Alvarez-Castro, M. C., and Yiou, P.: Dynamical properties and extremes of Northern Hemisphere climate fields over the past 60 years, NONLINEAR PROC GEOPH, 24, 713–725, https://doi.org/10.5194/npg-24-713-2017, 2017.

https://doi.org/10.5194/egusphere-2025-3664
Preprint. Discussion started: 8 August 2025

Feldstein, S. B. and Franzke, C. L. E.: Atmospheric Teleconnection Patterns, in: Nonlinear and Stochastic Climate Dynamics, chap. 3, pp. 54–104, Cambridge University Press, https://doi.org/10.1017/9781316339251.004, 2017.

Golian, S., Murphy, C., Wilby, R. L., Matthews, T., Donegan, S., Quinn, D. F., and Harrigan, S.: Dynamical–statistical seasonal forecasts of winter and summer precipitation for the Island of Ireland, INT J CLIMATOL, 42, 5714–5731, https://doi.org/10.1002/joc.7557, 2022.

Goutham, N., Plougonven, R., Omrani, H., Tantet, A., Parey, S., Tankov, P., Hitchcock, P., and Drobinski, P.: Statistical Downscaling to Improve the Subseasonal Predictions of Energy-Relevant Surface Variables, MON WEATHER REV, 151(1), 275–296, https://doi.org/10.1175/MWR-D-22-0170.1, 2023.

Hall, R. J., Wei, H.-L., and Hanna, E.: Complex systems modelling for statistical forecasting of winter North Atlantic atmospheric variability: a new approach to North Atlantic seasonal forecasting, Q J ROY METEOR SOC, 145(723), 2568–2585, https://doi.org/10.1002/qj.3579, 2019.

Hannachi, A.: Patterns Identification and Data Mining in Weather and Climate, Springer Atmospheric Sciences, https://doi.org/10.1007/978-3-030-67073-3, 2021.

Hannachi, A., Straus, D. M., Franzke, C. L. E., Corti, S., and Woollings, T.: Low-frequency nonlinearity and regime behavior in the Northern Hemisphere extratropical atmosphere, REV GEOPHYS, 55(1), 199–234, https://doi.org/10.1002/2015RG000509, 2017.

Hernanz, A., Carlos Correa, C., Juan-Carlos Sánchez-Perrino, J.-C., Prieto-Rico, I., Rodríguez-Guisado, E., Domínguez, M., and Rodríguez-Camino, E.: On the limitations of deep learning for statistical downscaling of climate change projections: The transferability and the extrapolation issues, ATMOS SCI LETT, 25(2), e1195, https://doi.org/10.1002/asl.1195, 2024.

Hersbach, H., Bell, B., Berrisford, P., and et al.: The ERA5 global reanalysis, Q J ROY METEOR SOC, 146(730), 1999–2049, https://doi.org/10.1002/qj.3803, 2020.

Høsskuldson, A.: PLS Regression Methods, J CHEMOMETR, 2, 211–228, https://doi.org/10.1002/cem.1180020306, 1988.

Kochkov, D., Yuval, J., Langmore, I., and et al.: Neural general circulation models for weather and climate, Nature, 632, 1060–1066, https://doi.org/10.1038/s41586-024-07744-y, 2024.

Kolstad, E. and O'Reilly, C.: Causal oceanic feedbacks onto the winter NAO, CLIM DYN, 62, 4223–4236, https://doi.org/10.1007/s00382-024-07128-y, 2024.

Lledó, L., Torralba, V., Soret, A., Ramón, J., and Doblas-Reyes, F. J.: Seasonal forecasts of wind power generation, RENEW ENERG, 143, 91–100, https://doi.org/10.1016/j.renene.2019.04.135, 2019.

Orlov, A., Sillmann, J., and Vigo, I.: Better seasonal forecasts for the renewable energy industry, NAT ENERG, 5(2), 108–110, https://doi.org/10.1038/s41560-020-0561-5, 2020.

Patrizio, C., Athanasiadis, P., Smith, D., and Nicolì, D.: Ocean-atmosphere feedbacks key to NAO decadal predictability, NPJ CLIM ATMOS SCI, 8, 146, https://doi.org/10.1038/s41612-025-01027-7, 2025.

Patterson, M., O'Reilly, C., Robson, J., and Woollings, T.: Disentangling North Atlantic Ocean–Atmosphere Coupling Using Circulation Analogs, J CLIMATE, 37(14), 3791–3805, https://doi.org/10.1175/JCLI-D-23-0602.1, 2024.

Perez, J., Maycock, A. C., Griffiths, S. D., Hardiman, S. C., and McKenna, C. M.: A new characterisation of the North Atlantic eddy-driven jet using two-dimensional moment analysis, WEATHER CLIM DYNAM, 5(3), 1061–1078, https://doi.org/10.5194/wcd-5-1061-2024, 2024.

Ramón, J., Lledó, L., Bretonnière, P.-A., Samsó, M., and Doblas-Reyes, F. J.: A perfect prognosis downscaling methodology for seasonal prediction of local-scale wind speeds, ENVIRON RES LETT, 16, 054 010, https://doi.org/https://doi.org/10.1088/1748-9326/abe491, 2021.

https://doi.org/10.5194/egusphere-2025-3664
Preprint. Discussion started: 8 August 2025

Rodríguez-Guisado, E., Serrano-de la Torre, A. A., Sánchez-García, E., Marta Domínguez-Alonso, M., and Ernesto Rodríguez-Camino, E.: Development of an empirical model for seasonal forecasting over the Mediterranean, ADV SCI RES, 16, 191–199, https://doi.org/10.5194/asr-16-191-2019, 2019.

Rosipal, R. and Krämer, N.: Overview and Recent Advances in Partial Least Squares, in: Saunders, C., Grobelnik, M., Gunn, S., Shawe-Taylor, J. (eds) Subspace, Latent Structure and Feature Selection. SLSFS 2005. Lecture Notes in Computer Science, vol 3940. Springer, Berlin, Heidelberg, p. 34–51, https://doi.org/10.1007/11752790_2, 2006.

Rouges, E., Ferranti, L., Kantz, H., and Pappenberger, F.: Pattern-based forecasting enhances the prediction skill of European heatwaves into the sub-seasonal range, CLIM DYN, 62(9), 9269–9285, https://doi.org/10.1007/s00382-024-07390-0, 2024.

Sánchez-García, E., Voces-Aboy, J., Navascués, B., and Rodríguez-Camino, E.: Regionally improved seasonal forecast of precipitation through Best estimation of winter NAO, ADV SCI RES, 19, 165–174, https://doi.org/10.5194/asr-16-165-2019, 2019.

Scaife, A. A. and Smith, D.: A signal-to-noise paradox in climate science, NPJ CLIM ATMOS SCI, 1, 28, https://doi.org/10.1038/s41612-018-0038-4, 2018.

Schuhen, N., Schaller, N., Bloomfield, H. C., Brayshaw, D. J., Lledó, L., Cionni, I., and Sillmann, J.: Predictive skill of teleconnection patterns in twentieth century seasonal hindcasts and their relationship to extreme winter temperatures in Europe, GEOPHYS RES LETT, 49, e2020GL092 360, https://doi.org/10.1029/2020GL092360, 2022.

Simpson, I., Hanna, E., Baker, L., Sun, Y., and Wei, H.-L.: North Atlantic atmospheric circulation indices: Links with summer and winter temperature and precipitation in North-West Europe, including persistence and variability, INT J CLIMATOL, 44(3), 902–922, https://doi.org/10.1002/joc.8364, 2024.

Simpson, I. R., Yeager, S. G., McKinnon, K. A., and Deser, C.: Decadal predictability of late winter precipitation in Western Europe through an ocean–jet stream connection, NAT GEOSCI, 12, 613–619, https://doi.org/10.1038/s41561-019-0391-x, 2019.

Spuler, F. R., Kretschmer, M., Kovalchuk, Y., Balmaseda, M. A., and Shepherd, T. G.: Identifying probabilistic weather regimes targeted to a local-scale impact variable, Environmental Data Science, 3, e25, https://doi.org/10.1017/eds.2024.29, 2024.

Strommen, K., Chantry, M., Dorrington, J., and Nina Otter, N.: A topological perspective on weather regimes, CLIM DYN, 60(5-6), 1415–1445, https://doi.org/10.1007/s00382-022-06395-x, 2022.

Strommen, K., Woollings, T., Davini, P., Ruggieric, P., and Simpson, I. R.: Predictable decadal forcing of the North Atlantic jet speed by sub-polar North Atlantic sea surface temperatures, WEATHER CLIM DYNAM, 4(4), 853–874, https://doi.org/10.5194/wcd-4-853-2023, 2023.

Sun, Y., Simpson, I., Wei, H.-L., and Hanna, E.: Probabilistic seasonal forecasts of North Atlantic atmospheric circulation using complex systems modelling and comparison with dynamical models, METEOROL APPL, 31(1), e2178, https://doi.org/10.1002/met.2178, 2024.

Tsartsali, E. E., Athanasiadis, P. J., Materia, S., Bellucci, A., Nicolì, D., and Gualdi, S.: Predicting precipitation on the decadal timescale: A prototype climate service for the hydropower sector, Climate Services, 32, 100 422, https://doi.org/10.1016/j.cliser.2023.100422, 2023.

Tyagi, A., Muhammad, A., Wandel, J., Dalelane, C., Happ, A., Paxian, A., Pauscher, L., and Siefert, M.: Developing Seasonal Wind Energy Forecasts for Germany, in: ECMWF Annual Seminar 2025, Bonn, Germany, 7-11 April 2025, https://events.ecmwf.int/event/418/contributions/4942/attachments/2917/4986/AS2025_Tyagi.pdf, 2025a.

Tyagi, A., Muhammad, A., Wandel, J., Happ, A., Paxian, A., Pauscher, L., Braun, M., and Siefert, M.: Evaluating the skill of seasonal forecasts in Germany, in: 2025 21st International Conference on the European Energy Market (EEM), Lisbon, Portugal, 27-29 May 2025, https://doi.org/10.1109/EEM64765.2025.11050088, 2025b.

https://doi.org/10.5194/egusphere-2025-3664
Preprint. Discussion started: 8 August 2025

Watt-Meyer, O., Dresdner, G., McGibbon, J., Clark, S. K., Henn, B., Duncan, J., Brenowitz, N. D., Kashinath, K., Pritchard, M. S., Bonev, B., Peters, M. E., and Bretherton, C. S.: ACE: A fast, skillful learned global atmospheric model for climate prediction, https://arxiv.org/abs/2310.02074, 2023.

West, H., White, P., Quinn, N., and Horswell, M.: The Spatio-Temporal Influence of Atmospheric Circulations on Monthly Precipitation in Great Britain, ATMOSPHERE-BASEL, 13(3), 429, https://doi.org/10.3390/atmos13030429, 2022.

Wold, H.: 11 - Path Models with Latent Variables: The NIPALS Approach, in: Blalock, H.M., Aganbegian, A., Borodkin, F.M., Boudon, R., Capecchi, V. (eds) Quantitative Sociology, pp. 307–357, Academic Press, ISBN 978-0-12-103950-9, https://doi.org/https://doi.org/10.1016/B978-0-12-103950-9.50017-4, 1975.